



OPEN ACCESS

EDITED BY

James Butcher,
University of Ottawa, Canada

REVIEWED BY

Vijay Antharam,
Methodist University, United States
Zhengwei Huang,
Shanghai Jiao Tong University, China

*CORRESPONDENCE

Yongxiang Yi

✉ ian0126@126.com

Heiyong Jin

✉ jinheiyong@yahoo.com

RECEIVED 21 February 2023

ACCEPTED 02 May 2023

PUBLISHED 16 May 2023

CITATION

Li X, Yi Y, Wu T, Chen N, Gu X, Xiang L, Jiang Z, Li J and Jin H (2023) Integrated microbiome and metabolome analysis reveals the interaction between intestinal flora and serum metabolites as potential biomarkers in hepatocellular carcinoma patients.

Front. Cell. Infect. Microbiol. 13:1170748.

doi: 10.3389/fcimb.2023.1170748

COPYRIGHT

© 2023 Li, Yi, Wu, Chen, Gu, Xiang, Jiang, Li and Jin. This is an open-access article distributed under the terms of the [Creative Commons Attribution License \(CC BY\)](https://creativecommons.org/licenses/by/4.0/). The use, distribution or reproduction in other forums is permitted, provided the original author(s) and the copyright owner(s) are credited and that the original publication in this journal is cited, in accordance with accepted academic practice. No use, distribution or reproduction is permitted which does not comply with these terms.

Integrated microbiome and metabolome analysis reveals the interaction between intestinal flora and serum metabolites as potential biomarkers in hepatocellular carcinoma patients

Xiaoyue Li^{1,2}, Yongxiang Yi^{1,2,3*}, Tongxin Wu¹, Nan Chen¹, Xinyu Gu², Liangliang Xiang², Zhaodi Jiang², Junwei Li¹ and Heiyong Jin^{4*}

¹Department of Infectious Diseases, The Second Hospital of Nanjing, Nanjing University of Chinese Medicine, Nanjing, China, ²Department of Hepatobiliary Surgery, The Second Hospital of Nanjing, Nanjing University of Chinese Medicine, Nanjing, China, ³Department of Hepatobiliary Surgery, Nanjing Drum Tower Hospital, Nanjing, China, ⁴Department of Colorectal Surgery, The Second Affiliated Hospital of Nanjing University of Chinese Medicine, Nanjing, China

Globally, liver cancer poses a serious threat to human health and quality of life. Despite numerous studies on the microbial composition of the gut in hepatocellular carcinoma (HCC), little is known about the interactions of the gut microbiota and metabolites and their role in HCC. This study examined the composition of the gut microbiota and serum metabolic profiles in 68 patients with HCC, 33 patients with liver cirrhosis (LC), and 34 healthy individuals (NC) using a combination of metagenome sequencing and liquid chromatography–mass spectrometry (LC–MS). The composition of the serum metabolites and the structure of the intestinal microbiota were found to be significantly altered in HCC patients compared to non-HCC patients. LEfSe and metabolic pathway enrichment analysis were used to identify two key species (*Odoribacter splanchnicus* and *Ruminococcus bicirculans*) and five key metabolites (ouabain, taurochenodeoxycholic acid, glycochenodeoxycholate, theophylline, and xanthine) associated with HCC, which then were combined to create panels for HCC diagnosis. The study discovered that the diagnostic performance of the metabolome was superior to that of the microbiome, and a panel comprised of key species and key metabolites outperformed alpha-fetoprotein (AFP) in terms of diagnostic value. Spearman's rank correlation test was used to determine the relationship between the intestinal flora and serum metabolites and their impact on hepatocarcinogenesis and progression. A random forest model was used to assess the diagnostic performance of the different histologies alone and in combination. In summary, this study describes the characteristics of HCC patients' intestinal flora and serum metabolism, demonstrates that HCC is caused by the interaction of intestinal flora and serum metabolites, and

suggests that two key species and five key metabolites may be potential markers for the diagnosis of HCC.

KEYWORDS

intestinal flora, serum metabolites, biomarkers, hepatocellular carcinoma, integrated analysis

Introduction

Primary liver cancer is the fourth leading cause of cancer-related deaths worldwide, with hepatocellular carcinoma (HCC) accounting for approximately 80% of all cases (Bray et al., 2018). China represents approximately half of all new cases and deaths related to HCC worldwide (Torre et al., 2015). Although surgery can help patients with liver cancer, the 5-year survival rate is only 50%–70% (2022). Furthermore, most HCC patients are diagnosed in advanced stages with a poor prognosis due to a lack of specific symptoms in the early stages and no known early diagnostic markers (Kobayashi et al., 2017). To screen for and diagnose HCC, imaging methods (e.g., CT and B-ultrasound) and serum biomarkers (e.g., AFP) are commonly used. However, imaging alone is insufficient for distinguishing small HCCs from hepatic sclerosing nodules. In addition, AFP has a sensitivity of 65% for the clinical diagnosis of HCC and a sensitivity of less than 40% for preclinical prediction (Marrero and Lok, 2004). As a result, new biomarkers and effective drug targets are urgently needed to improve the prognosis of HCC patients.

Gut microbes and circulating metabolites have received much attention as biomarkers for human diseases such as cancer in recent years due to the development and application of sequencing technologies and LC–MS-based metabolomics. Intestinal microbes are recognized as novel virtual metabolic organs, and the gut microbiota has been demonstrated to play a significant role in the development of numerous diseases. By altering the permeability of the intestinal mucosa in a way that disrupts immune or metabolic homeostasis, gut microbiota imbalances can contribute to the development of autoimmune diseases or cancer (Qin et al., 2012; Dodd et al., 2017; Lucas et al., 2017). The close relationship between the liver and the intestine is referred to as the “gut-liver axis” (Tripathi et al., 2018). An intact gut-liver axis is dependent on a healthy intestinal microbiota and normal liver function. In addition, the gut microbiota has been identified as an important player in chronic inflammatory liver disease, liver cirrhosis, alcoholic liver disease, and nonalcoholic fatty liver disease (Bajaj et al., 2014; Shen et al., 2017; Ponziani et al., 2019). Several studies have shown that the gut microbiota can be used as a noninvasive diagnostic tool for certain diseases and cancers, such as type 2 diabetes (T2D), colorectal cancer (CRC), and pancreatic cancer (PC) (Ren et al., 2017; Yu et al., 2017). Although the importance of microbes in HCC has been reported in several studies, the profile of the gut microbial community and its functional contribution to HCC has yet to be thoroughly studied

and systematically characterized (Ren et al., 2019; Huang et al., 2020).

Using microbial metabolites, the gut microbiota has been linked to diseases such as cancer (Louis et al., 2014). Food and nutrients are transformed by gut microbes into a metabolite environment, which controls the equilibrium of the metabolites (Anand et al., 2016). By providing metabolic flux to promote anabolism, acting as competitive enzyme inhibitors, or modifying signaling proteins, among other mechanisms, these metabolites can exert genotoxic or tumor-suppressive effects (O’Keefe, 2016).

The liver is one of the most active metabolizing organs in our bodies, and it plays an important role in regulating various metabolic processes (Fausto et al., 2006). The liver receives metabolites produced by bacteria in the gut via the portal vein and transports them directly to the liver to perform regulatory functions. Because of the natural connection between intestinal microbes and the liver, the liver is the first organ to receive intestinal metabolites and it plays an essential role in the interaction between extraneous materials and the systemic environment. Metabolomics is a very promising method for identifying metabolites that can shed light on the etiology, treatment, and early diagnosis of disease (Beyoğlu and Idle, 2013).

The process of tumorigenesis is accompanied by an overall shift in metabolic status, which has an effect not only on the tissue of the tumor but also on the microenvironment surrounding it (Al-Zoughbi et al., 2014; Vander Heiden and DeBerardinis, 2017). Furthermore, metabolic changes can be observed more directly in the tumor cell state than genomic and proteomic changes and are thus expected to become useful tumorigenesis biomarkers (Patel and Ahmed, 2015). In the past few years, much research has been done on the metabolites in the blood that are linked to liver cancer. This research has shown that metabolites play a major role in the development of HCC (Tong et al., 2021; Liu et al., 2022).

With increasing research on the gut microbiome and metabolome as biomarkers in HCC, we have a deeper understanding of possible diagnostic methods for HCC. However, little is known about the interactions between gut microbes and metabolites and how they influence the development of liver cancer. In this study, metagenome sequencing of stool and metabolomic analysis of serum from three cohorts (HCC, LC, and NC) were performed to discover changes in gut microbes and serum metabolites. Simultaneously, matched serum and stool samples were analyzed for metabolites and microbes, and it was discovered that gut microbes were closely associated with serum metabolites. Based on these findings, the diagnostic performance of

key gut microbes, key serum metabolites, and key gut microbial metabolites were compared. Meanwhile, the molecular pathway mechanisms were examined to learn more about hepatocarcinogenesis.

Materials and methods

Participant information

This study included 68 newly diagnosed hepatocellular carcinoma patients, 33 patients with liver cirrhosis from the Hepatobiliary and Pancreatic Treatment Center of the Second Hospital of Nanjing, Jiangsu Province, and 34 healthy subjects from the Health Management Center. Stool and serum samples were collected in accordance with the protocol approved by the ethics committee of the Second Hospital of Nanjing, and all participants provided written informed consent. The study subjects' demographic and clinical data, CT scans, and dietary habits were obtained from hospital electronic medical records and questionnaires (online [Supplementary Table S1](#)). International guidelines say that HCC or cirrhosis can be diagnosed by looking at integrated pathology, imaging, laboratory tests, clinical symptoms, and medical history.

The HCC patients were screened and confirmed. The following were the exclusion criteria: 1) patients with other diseases, such as tumors in other locations, gastrointestinal diseases, hypertension, diabetes, and metabolic diseases; 2) patients who had previously received anticancer treatment; 3) patients who had recently received antibiotics or probiotics; and 4) patients who lacked critical clinical information. Age, sex ratio, BMI, and dietary habits were used to match the patients with the controls. Individuals who had hypertension, diabetes, obesity, metabolic syndrome, irritable bowel syndrome (IBD), or had received antibiotics and/or probiotics treatment within the previous 8 weeks were also excluded.

Sample collection

Fresh fecal samples were collected from each participant and evaluated for fecal morphology and color. The samples were divided into three 300 mg portions and immediately snap-frozen in liquid nitrogen. The entire process of moving and manipulating the samples on ice took less than 20 minutes. After snap-freezing with liquid nitrogen, the samples were stored at -80°C until extraction for testing. A professional nurse collected venous blood in strict accordance with standard asepsis procedures. The serum was centrifuged and stored at -80°C until testing.

Microbial DNA extraction, metagenome sequencing and data processing

Total DNA was extracted from the stool samples using the QIAamp 96 Power Fecal QIAcube HT kit (Qiagen, Germany), and

the DNA was further purified using the MGI Easy DNA Magnetic Beads Purification Kit (MGI, China) according to the manufacturer's instructions. To measure how much purified DNA there was, a Qubit dsDNA BR Assay Kit (Invitrogen, USA) was used.

The library was built using DNBSEQ (online [Supplementary Figure S1](#)) and the original sequencing data (Raw Data) were filtered using the short oligonucleotide alignment program SOAP (Li et al., 2008) to obtain clean data, and the host sequence was aligned with Bowtie2 (Langmead and Salzberg, 2012) to remove reads derived from the host. MEGAHIT (Li et al., 2015) assembled high-quality short reads from each DNA sample. MetaGeneMark (Zhu et al., 2010) was used to perform metagenomic gene prediction on the assembled scaffold. CD-HIT (Fu et al., 2012) was used to cluster predicted genes, and redundant sequences were removed to construct the gene catalog. Salmon (Patro et al., 2017) was used for quantification. Diamond's (Buchfink et al., 2015) BLASTP function was used for functional annotation, and Kraken2's default parameters were used for taxonomic annotation.

LC/MS nontargeted metabolomics analysis

Metabolite extraction was performed according to a previously reported method. In short, samples were extracted by directly adding precooled methanol and acetonitrile (2:1, v/v), and internal standards mix 1 (IS1) and internal standards mix 2 (IS2) were added for quality control of the sample preparation. After vortexing for 1 minute and incubating at -20°C for 2 hours, the samples were centrifuged for 20 minutes at 4000 rpm, and the supernatant was then transferred for vacuum freeze drying. The metabolites were resuspended in 150 μL of 50% methanol and centrifuged for 30 min at 4000 rpm, and the supernatants were transferred to autosampler vials for LC-MS analysis. A quality control (QC) sample was prepared by pooling the same volume of each sample to evaluate the reproducibility of the whole LC-MS analysis. For metabolite separation and detection, a Waters 2D UPLC (Waters, USA) tandem Q Exactive high-resolution mass spectrometer (Thermo Fisher Scientific, USA) was used. The samples were analyzed using a Waters 2D UPLC (Waters, USA) coupled to a Q-Exactive mass spectrometer (Thermo Fisher Scientific, USA) with a heated electrospray ionization (HESI) source and that was controlled by the Xcalibur 2.3 software program (Thermo Fisher Scientific, Waltham, MA, USA). The separation was carried out on a Waters ACQUITY UPLC BEH C18 column (1.7 m, 2.1 mm, 100 μm , Waters, USA), with the column temperature set to 45°C . In positive mode, the mobile phase contained 0.1% formic acid (A) and acetonitrile (B), while in negative mode, the mobile phase contained 10 mM ammonium formate (A) and acetonitrile (B). The gradient conditions were as follows: 0–1 min, 2% B; 1–9 min, 2%–98% B; 9–12 min, 98% B; and 12.1–15 min, 2% B. The injection volume was 5 μL , and the flow rate was 0.35 mL/min. Compound Discoverer 3.1 (Thermo Fisher Scientific, USA) software was used to process the LC-MS/MS data, which included peak extraction, peak alignment, and compound identification (Dunn et al., 2011; Sarafian et al., 2014).

Statistical analysis

To compare the differences between different microorganisms, the Wilcoxon rank-sum test, Kruskal–Wallis (K–W), LEfSe analysis, Adonis and ANOSIM were used (Stat et al., 2013). The metabolomics R package metaX (Wen et al., 2017) and the metabolome bioinformatic analysis pipeline were used for data preprocessing, statistical analysis, metabolite classification annotations, and functional annotations. To compare metabolites between groups, principal component analysis (PCA), partial least squares discriminant analysis (PLS-DA), Student's t test, and fold change obtained from the variability analysis were used. The correlation between microorganisms and metabolites was evaluated using Spearman correlation and random forest analyses. Pearson correlation analysis was used to evaluate the correlation of species and metabolites with the clinical data. The statistical significance level was set at $p < 0.05$.

Results

After a rigorous pathological diagnosis and exclusion process, 68 patients with HCC, 33 patients with LC, and 34 NC were included in the analysis and comparison. Metagenome sequencing and untargeted LC–MS analysis were performed on the feces and serum of the participants, respectively. K–W, the Wilcoxon rank-sum test, and abundance restriction were used to screen different subgroups of microbes, and LEfSe analysis was used to screen HCC-associated species-level key gut microbiota (KGM). In addition, a metabolic pathway enrichment analysis was performed on the differential metabolites that were screened

based on the untargeted LC–MS results to screen for HCC-related key serum metabolites (KSM) in important metabolic pathways. Using random forest classification models, the potential of various panels consisting of different species or metabolites as biomarkers was evaluated. Then, in fecal- and serum-matched enrollees, a combined analysis of differential species and differential metabolites was performed to determine which omics best separated HCC from non-HCC by comparing separate and combined modeling of different omics with the receiver operating characteristic (ROC) curves. Finally, the best panel's worth was determined by comparing the difference between the best panel and the best omics model (Figure 1).

Demographics of the study cohort and quality control of the samples

Before the experimental design and sample collection, participants were matched for dietary habits and clinical characteristics (including age, sex, and body mass index) to ensure that established confounding factors did not affect group differentiation. Serum levels of alanine aminotransferase (ALT), aspartate aminotransferase (AST), glutamyl transpeptidase (GGT), and total bilirubin were significantly higher in HCC patients than in controls, but total protein and platelets were significantly lower (Table 1).

Stool morphology and color were assessed prior to metagenome sequencing. Except for one stool sample with an abnormal color in the HCC group, all stool samples were yellow and soft, with no significant differences among the groups (online Supplementary Table S2). To ensure the accuracy of the subsequent analysis, the

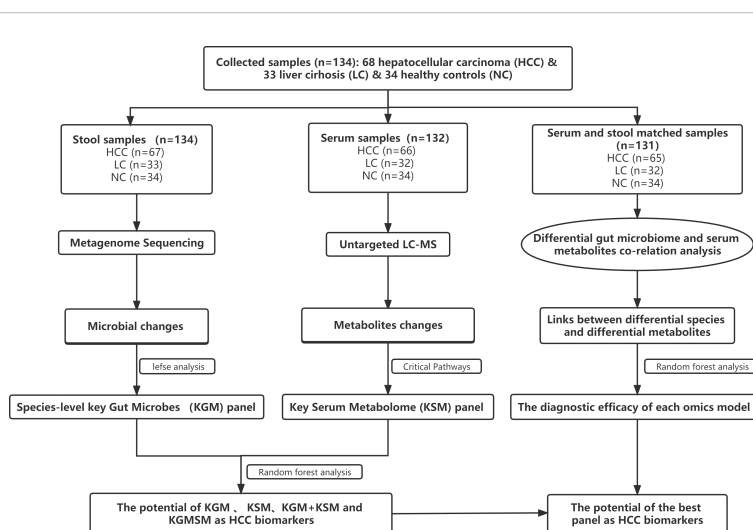


FIGURE 1

A schematic of the design and the experimental flow diagram. After a strict pathological diagnosis and exclusion process, 68 patients with HCC, 33 patients with cirrhosis, and 34 healthy controls were included at the Second Hospital of Nanjing, Jiangsu Province, China. In total, 132 serum samples and 134 feces samples were included in the analysis. Characterized the gut microbiome of 67 patients with HCC, 33 patients with cirrhosis, and 34 healthy controls and identified the microbial markers. Simultaneously characterized the serum metabolites from 66 hepatocellular carcinomas, 32 cases of hepatic sclerosis, and 34 healthy controls to identify metabolite markers. Random forest analysis is used to assess the ability of various marker combinations to distinguish the HCC cohort from the non-HCC cohort (cirrhosis and healthy controls). Using serum- and fecal-matched cohorts to examine the link between the gut microbiota and serum metabolites that changed significantly in HCC. HCC, hepatocellular carcinoma; KGM, key gut microbes; KSM, key serum metabolites; KGMSM, key gut microbial-associated serum metabolites.

raw sequencing data from 134 stools (67 HCC, 33 LC, and 34 NC) were filtered and assembled for statistical analysis and gene prediction (online Supplementary Table S3).

After the removal of hemolyzed serum samples, a total of 132 serum samples (66 HCC, 32 LC, and 34 NC) were included in the analysis (online Supplementary Table S1). The base peak chromatograms (BPC) of all QC samples overlapped, the spectrum overlap was good, and the retention time and peak response intensity fluctuated very little, indicating that the instrument was in good condition and that the signal was stable throughout the entire sample detection and analysis (online Supplementary Figure S2A). The ratio of compounds in the QC sample with a relative peak area coefficient of variation (CV) of less than or equal to 30% to the total number of compounds was higher than 60%, indicating that the data quality was sufficient (online Supplementary Figure S2B).

Intestinal flora structural changes in hepatocellular carcinoma

Statistical analyses of microbial abundance for each of the three groups were conducted. The estimated species richness in each

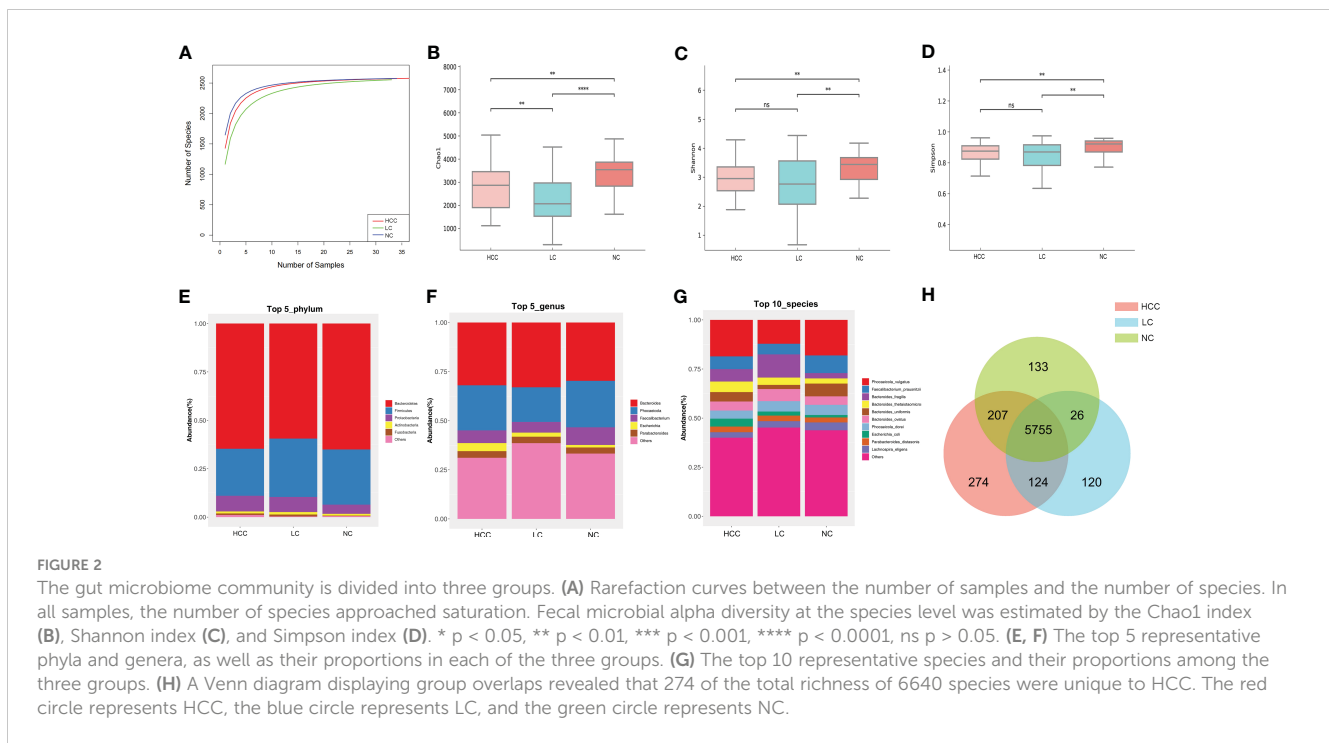
group was close to saturation according to the rarefaction analysis (Figure 2A). The Chao1 indices of the different groups differed significantly at both the phylum and genus levels, whereas the Shannon and Simpson indices differed significantly at the genus level but not at the phylum level (online Supplementary Figure S3). At the species level (online Supplementary Table S4), the Chao1 indices revealed that the community richness differed significantly among the groups, with NC > HCC > LC (Figure 2B); Shannon indices and Simpson indices demonstrated that the microbiome diversity of HCC and LC was significantly lower than that of NC, with the diversity of HCC being higher than that of LC (with no significance) (Figures 2C, D).

The structure of the intestinal flora communities of the three groups were investigated in this study (online Supplementary Table S5). Bacteroidetes, Firmicutes, and Proteobacteria accounted for more than 90% of the total abundance and were the dominant phyla in the three groups (Figure 2E). At the genus level, Bacteroides and Phocaeicola were the most dominant in all three groups, with the relative abundance of Bacteroides increasing and Phocaeicola decreasing in HCC and LC compared to NC (Figure 2F). At the species level, except for *Phocaeicola vulgatus*, which had the highest abundance in all three groups, the most abundant species in HCC were *Faecalibacterium prausnitzii* (6.48%), *Bacteroides fragilis*

TABLE 1 Clinical characteristics of the enrolled participants.

Clinical and pathological indexes				P values (NC vs. HCC)	P values (LC vs. HCC)
	NC (n=34)	LC (n=33)	HCC (n=68)		
Age (year)	55.50±8.66	54.18±11.49	57.88±9.97	0.068	0.138
Gender					
Female	13(38%)	8(24%)	15(22%)	0.087	0.811
Male	21(62%)	25(76%)	53(78%)		
BMI	22.71±1.24	22.78±1.27	22.89±1.31	0.441	0.712
AFP (ng/mL)					
≤20	34(100%)	27(82%)	37(54%)	<0.0001	0.008
>20	0	6(18%)	31(46%)		
ALT (0–40 U/L)	22.11±13.89	38.42±40.09	72.61±139.03	0.0002	0.172
AST (0–40 U/L)	19.64±5.11	43.61±27.14	86.63±146.22	<0.0001	0.555
GGT (0–40 U/L)	24.02±14.05	78.28±96.53	103.22±139.75	<0.0001	0.438
Total protein (66.0–87.0 g/L)	72.22±3.47	63.24±8.52	64.07±6.74	<0.0001	0.567
Total bilirubin (3.0–19.0 umol/L)	10.55±3.88	37.73±33.19	24.94±26.17	<0.0001	0.016
Platelets (101–320 10 ⁹ /L)	254.00±63.11	86.27±69.39	127.04±74.51	<0.0001	0.002
Aetiological factors					
HBV	NA	28(85%)	61(90%)	–	0.485
others	NA	5(15%)	7(10%)		
Dietary habit	Mixed diet	Mixed diet	Mixed diet		

One-way analysis of variance was used to evaluate the differences among the three groups. The Wilcoxon rank-sum test was used to compare the variables between the two groups. BMI, body mass index; AFP, alpha-fetoprotein; ALT, alanine aminotransferase; AST, aspartate aminotransferase; GGT, glutamyl transpeptidase; HBV, hepatitis B virus; HCC, hepatocellular carcinoma; LC, liver cirrhosis; NC, healthy controls; NA, not applicable; Mixed diet, the participants did not have picky or poor dietary habits, i.e., they were not pure vegetarians or pure meat eaters, and they were all from Nanjing, China, with roughly the same dietary habits.



(6.32%), and *Bacteroides thetaiotaomicron* (5.35%), and in LC, they were *Bacteroides fragilis* (11.8%), *Bacteroides ovatus* (6.14%), and *Faecalibacterium prausnitzii* (5.41%). Additionally, the most prevalent bacteria in NC were *Faecalibacterium prausnitzii* (8.99%), *Bacteroides uniformis* (6.51%), and *Phocaeicola dorei* (5.16%) (Figure 2G). Additionally, Venn plots of the intergroup overlap showed that 5755 of the 6640 species found were shared by all three groups, while 274 species were found only in HCC (Figure 2H).

Differential analysis of intestinal microbes

To compare the differences in fecal microbial communities between groups and to identify microbes associated with HCC, K–W was performed on HCC, LC, and NC, and microbes with a p value < 0.05 and median relative abundance greater than 0.01% of the total abundance were recognized as differential microbes. The results showed that a total of 4 phyla, 49 genera, and 86 species were identified ($p < 0.05$) (online Supplementary Table S6). The Wilcoxon rank-sum test was used to compare the differences in microbes among the groups (online Supplementary Figures S4A–C).

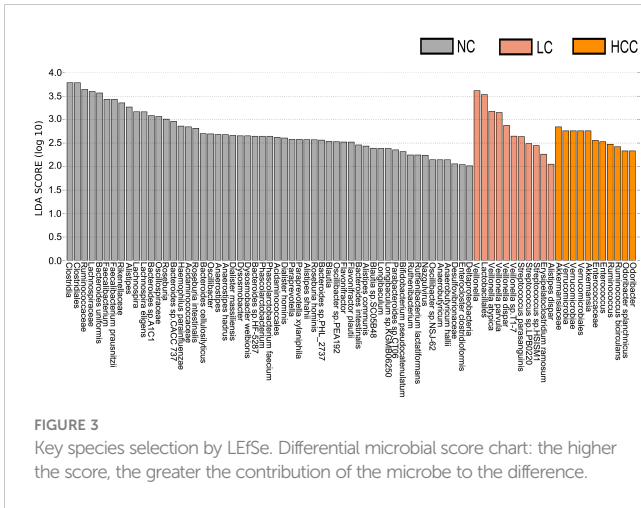
At the phylum level, the number of Verrucomicrobia was significantly higher in HCC patients than in LC patients, whereas Cyanobacteria, Euryarchaeota, and Uroviricota were lower in HCC patients than in NC patients ($p < 0.05$) (online Supplementary Table S7). At the genus level, 21 genera, including *Roseburia*, *Lachnospira*, and *Ruminococcus*, were significantly higher in HCC than LC, while 42 genera, excluding *Veillonella*, were significantly lower in HCC than NC, including *Faecalibacterium*, *Alistipes*, and

Phaeoalarctobacterium. (online Supplementary Table S8). Correspondingly, 35 species, such as *Phocaeicola vulgatus*, *Lachnospira eligens*, *Bacteroides uniformis*, and *Ruminococcus bicirculans*, differed between HCC and LC ($p < 0.05$). Compared to NC, except for *Veillonella parvula*, *Veillonella* sp. T1–7, *Veillonella atypica*, and *Veillonella dispar*, which were significantly increased in HCC, all 57 species (*Phocaeicola dorei*, *Bacteroides uniformis*, *Faecalibacterium prausnitzii*, etc.) were significantly reduced ($P < 0.05$) (online Supplementary Table S9). Furthermore, the bacterial differences between LC and NC at the phylum and species levels were compared, and the results as shown in (online Supplementary Tables S7–S9).

LEfSe was used to identify the key gut microbiota. After excluding species with relative abundances of less than 0.01%, the HCC, LC, and NC groups contained 2, 9, and 30 species, respectively (Figure 3). *Odoribacter splanchnicus* and *Ruminococcus bicirculans* were species-level potential biomarkers for the detection of HCC.

Serum metabolite changes in patients with hepatocellular carcinoma

Tumorigenesis is accompanied by a general change in the metabolite status of the local tissue and circulatory system. Metabolites and fermentation products produced by the intestinal flora can enter the bloodstream and impact the host's physiological functions. The metabolic profile in the serum was examined to investigate the relationship between metabolites in the serum and HCC. 8,709 ions were scanned by mass spectrometry, 2,934 of which were identifiable, which is the sum of metabolites detected in all samples and does not imply that they varied in various

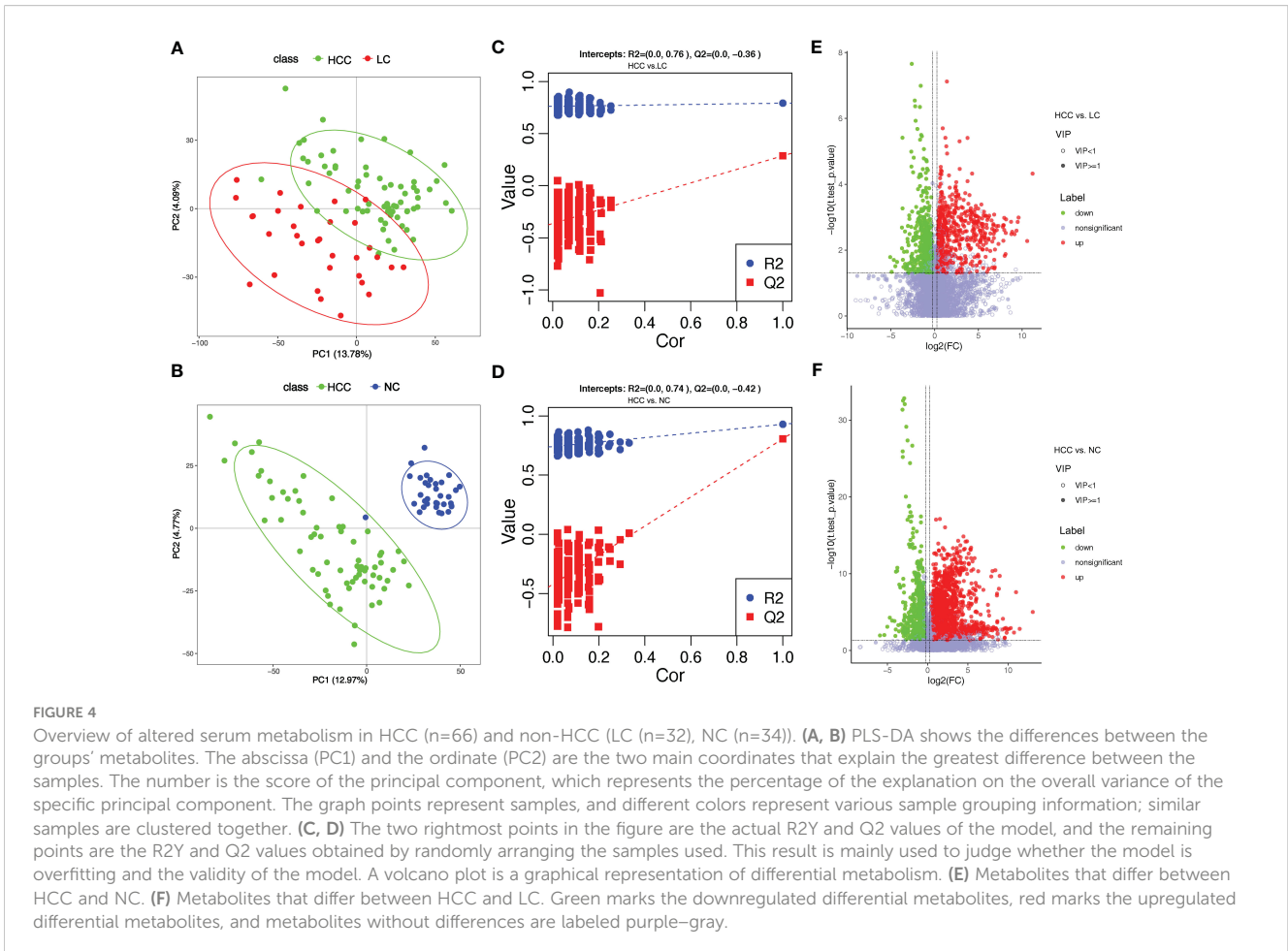


subgroups. (online [Supplementary Table S10](#)). Based on the abundance of metabolites detected by untargeted metabolomics, PLS-DA was performed ([Figures 4A, B](#)). According to the scatter plot, the samples from HCC, LC, and NC were separable, and the alignment test revealed that the data were not overfitted ([Figures 4C, D](#)) (in general, the closer the slopes of the R2Y and Q2Y lines are to zero, the more likely the model is overfitted). The

PLS-DA analysis for LC versus NC is depicted in online [Supplementary Figures S5A, B](#).

PLS-DA yielded “Variable Importance in Projection” (VIP) values, with larger values indicating a greater contribution of the variable to the subgroup. The following criteria were used to screen biologically significant differential metabolites: 1) VIP value ≥ 1 for the PLS-DA’s first principal component, 2) p value < 0.05 for the t test, and 3) fold-change ≥ 1.2 or ≤ 0.83 . In HCC versus LC, HCC versus NC, and LC versus NC, 424, 823, and 825 differential metabolites were screened for biological significance, respectively (online [Supplementary Table S11](#)). The differences in metabolism between HCC and non-HCC were demonstrated using volcano plots ([Figures 4E, F](#)). The volcano plots of LC versus NC are shown in online [Supplementary Figure S5C](#).

To better understand the mechanism of differential metabolites implicated in the pathogenesis of HCC, metabolic pathway enrichment analysis was performed on the KEGG IDs of the differential metabolites. Metabolic pathways with p values less than 0.05 were considered to be significantly enriched in differential metabolites and plotted bubble plots ([Figures 5A–C](#)) for these pathways (the metabolites on the pathways are shown in online [Supplementary Table S12](#)). Bile secretion, cholesterol metabolism, purine metabolism, caffeine metabolism, metabolic pathways, apoptosis, and vitamin digestion and absorption were



all significantly enriched in the HCC versus LC comparison group. The pathways that were significantly enriched in the HCC versus NC comparison group included caffeine metabolism, metabolic pathways, bile secretion, cholesterol metabolism, primary bile acid biosynthesis, drug metabolism - other enzymes, prostate cancer, and porphyrin and chlorophyll metabolism. In the LC versus NC comparison group, the differential metabolites were involved in caffeine metabolism, bile secretion, cholesterol metabolism, primary bile acid biosynthesis, metabolic pathways, porphyrin and chlorophyll metabolism, and cysteine and methionine metabolism.

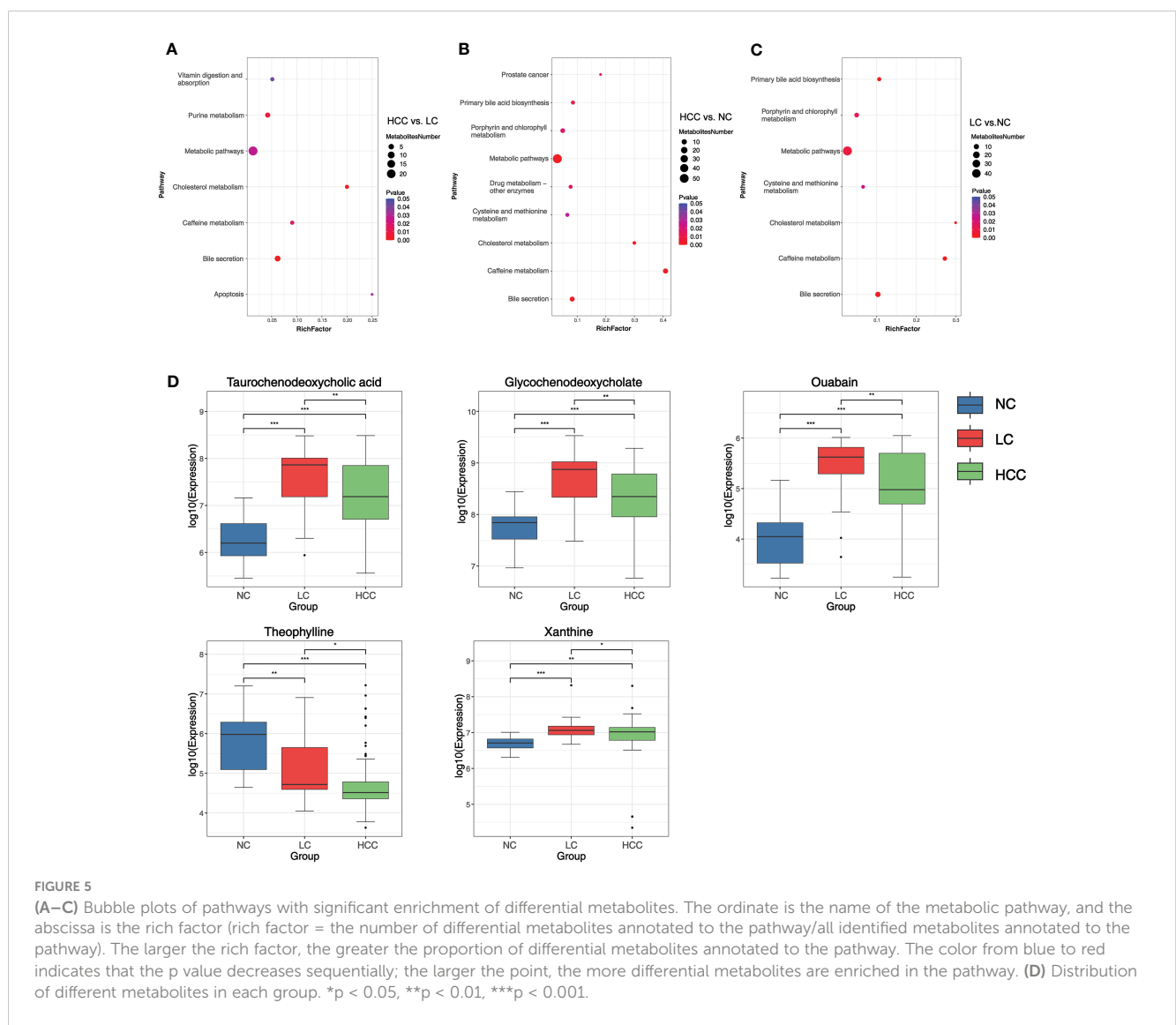
It was discovered that the bile secretion, cholesterol metabolism, and caffeine metabolism pathways are all associated with the progression of HCC. Three pathway-related differential metabolites involved in all three comparison groups were focused on to find metabolomic markers: ouabain, taurochenodeoxycholic acid (TCDCA), glycochenodeoxycholate (GCDCA), theophylline, and xanthine (online Supplementary Table S13). The expression of these metabolites in various groups were researched (Figure 5D). The findings revealed that the expression of ouabain, TCDCA, and GCDCA was significantly lower in HCC than in LC but significantly

higher than in NC. Theophylline expression was significantly lower in HCC compared to non-HCC, whereas xanthine expression was significantly higher in HCC compared to NC.

Correlation analysis of metagenome and metabolome

Correlation analysis and joint analysis of serum and fecal matched microbiome-metabolome data (65 in HCC, 32 in LC, and 34 in NC) were performed to explore the relationship between the microbiota and the serum metabolome. By calculating Spearman correlation coefficients between different species and metabolites, a correlation coefficient matrix was obtained (online Supplementary Table S14), as well as the top 20 differential species and metabolites with the smallest p values for each omics, which were chosen for the heatmap (Figures 6A, B), and the results of LC versus NC are shown in Supplementary Figure S6A.

The association analysis of *Odoribacter splanchnicus* and *Ruminococcus bicirculans* with differential metabolites was



performed to screen for key species-associated serum metabolites and discovered 66 key species with significantly associated metabolites in HCC versus LC and 45 in HCC versus NC ($p < 0.05$) (Online Supplementary Table S15). In both comparison groups, nine metabolites showed significant associations with key species associated with HCC, including three key metabolites (TCDCa, GCDCA, and xanthine) associated with HCC (Figure 7A).

By comparing the ROC curves between the separate modeling of different omics and the combined data modeling, which omics better separates HCC and non-HCC was evaluated, and it was discovered that in HCC versus LC, merged > species > metabolites with AUC values of 0.800, 0.708, and 0.696, respectively (Figure 7B). Metabolites > merged > species had AUC values of 1.000, 0.944, and 0.582 for HCC versus NC, respectively (Figure 7C). The results of LC versus NC are shown in Supplementary Figure S6B.

Evaluation of the contribution of various panels to the prediction of HCC using ROC curves

To evaluate the biomarker potential of HCC-related keystone species and metabolites, a key KGM panel with *Odoribacter splanchnicus* and *Ruminococcus bicirculans* and a KSM panel with ouabain, TCDCa, GCDCA, theophylline, and xanthine were constructed. Each panel's ability to distinguish between HCC and non-HCC were tested. Based on the relative abundance of metagenome and untargeted metabolic profile assays, the data from each panel were divided into a training set and a validation set, first building a random forest model for the training set and

then using this model to predict the validation set and construct ROC curves. 10-fold cross-validation was performed and then averaged the resulting ROC-curve. The AUC values of the KGM panel for HCC versus NC and HCC versus LC were 0.60 ± 0.22 and 0.65 ± 0.19 , respectively (Figure 8A), whereas the AUC values of the KSM panel for distinguishing HCC from NC and LC were 0.95 ± 0.06 and 0.65 ± 0.15 , respectively (Figure 8B). It is also worth noting that the KSM panel did surprisingly well to distinguish LC from the NC group (AUC: 0.93 ± 0.12) (online Supplementary Figure S5D). After that, we incorporated the KGM and KSM data into the random forest model to develop the ROC curve. The AUC values of the KGM+KSM panel for HCC versus NC and HCC versus LC were 0.97 ± 0.06 and 0.72 ± 0.18 , respectively (Figure 8C).

The clinical indicator AFP (cutoff value of 20 ng/mL) is commonly used to aid in the diagnosis of HCC. To compare the efficacy of AFP and our KGM+KSM panel in detecting HCC, AFP levels in all individuals included in this study were recorded. According to the findings, the AUC values for the AFP panel for HCC versus NC and LC were 0.75 ± 0.19 and 0.70 ± 0.19 , respectively (Figure 8D). In contrast, the KGM+KSM panel performed better than the AFP panel in terms of diagnostic value. When KGM+KSM was combined with AFP to build the ROC curve, the AUC values for distinguishing HCC from NC and LC improved slightly when compared to the KGM+KSM panel, reaching 0.99 ± 0.02 and 0.76 ± 0.17 , respectively (Figure 8E). Furthermore, it created a KGMSM (key gut microbial-associated serum metabolites) panel with 9 differential serum metabolites related to key species, which had significantly lower potential as HCC markers than the KGM+KSM panel, with AUC values of 0.86 ± 0.14 and 0.53 ± 0.18 for HCC versus NC and HCC versus LC, respectively (Figure 8F).

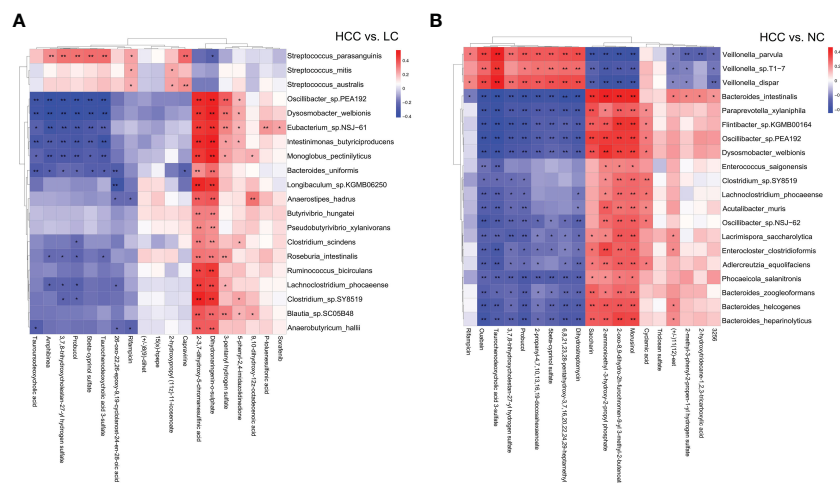


FIGURE 6 (A, B) The heatmap of the top 20 differential species and differential metabolites with the smallest p values for every omics in HCC vs. non-HCC. Columns represent the differential metabolites, and rows represent the differential species. The color blocks represent the correlation coefficient. The darker the color, the stronger the correlation between the different species and the different metabolites. Red represents a positive correlation, and blue represents a negative correlation. * represents $p < 0.05$, ** represents $p < 0.01$.

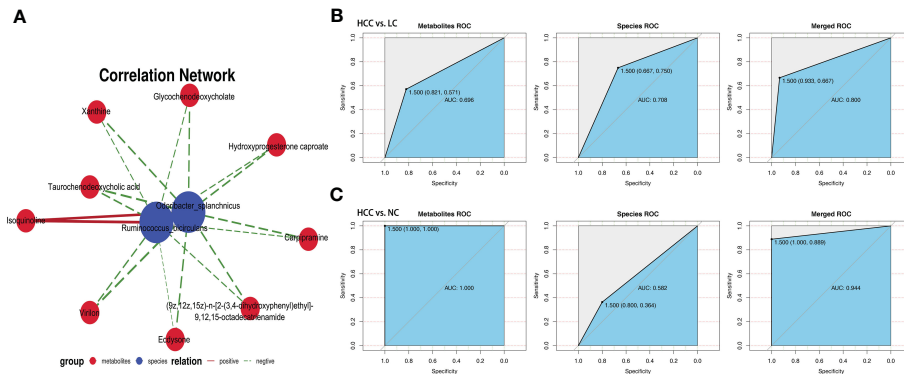


FIGURE 7 Correlation analysis of the metagenome and metabolome. **(A)** Spearman correlation network interaction diagram of the key species and differential metabolites. Each point in the figure represents a species or a metabolite. The more lines there are between the points, the more species or metabolites it may regulate. Blue dots represent species, red dots represent metabolites, red connecting lines between dots are positive correlations, and green lines are negative correlations. The thickness of the line represents the level of the correlation coefficient. **(B, C)** Random forest ROC map of species and metabolomes (the ROC map of the metabolome is on the left, the ROC map of species is in the middle, and the ROC map of the species and metabolomes is on the right).

Correlation of key species, key metabolites, and clinical indicators

Spearman correlation on key metabolites and key species associated with HCC was performed, and the results revealed that ouabain, TCDCA, GCDCA, and xanthine had a significant negative correlation with *Odoribacter splanchnicus* and *Ruminococcus*

birculans (Figure 9A). Meanwhile, Pearson correlation analysis of key species and key metabolites with AFP, liver function index, and immune cells were conducted (Figures 9B, C). *Odoribacter splanchnicus* was found to be significantly and positively correlated with AFP, white blood cells (WBCs), and leukocytes (LYs); GCDCA and TCDCA were significantly and positively correlated with total bilirubin (TBIL) and GGT but significantly and negatively

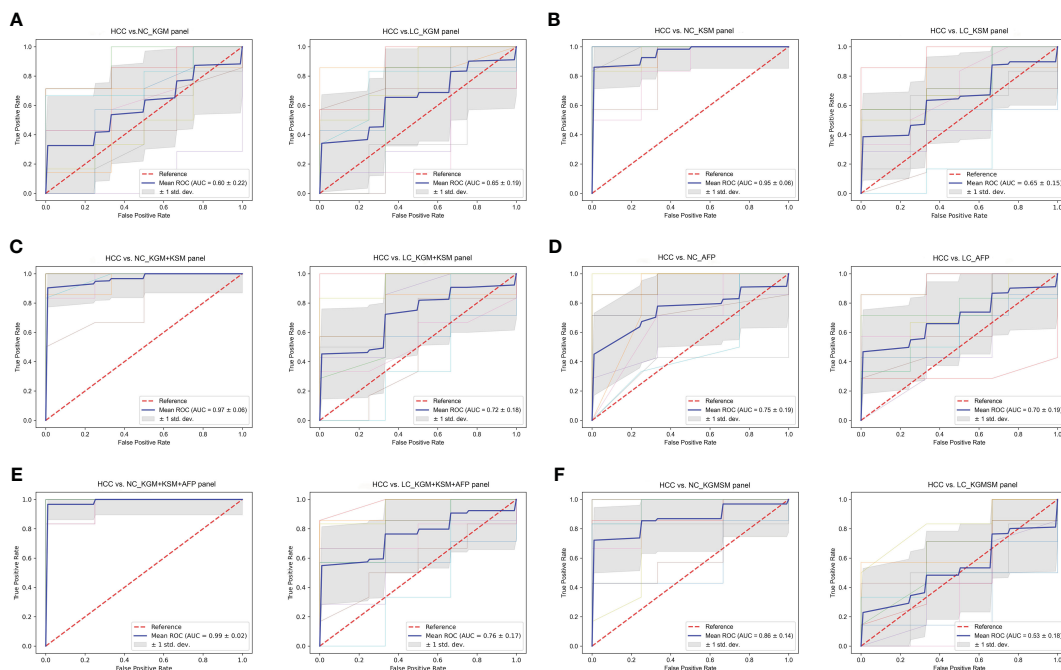


FIGURE 8 **(A–F)** The ROC curves of a random forest analysis of different panels. KGM, key gut microbes; KSM, key serum metabolites; KGMSM, key gut microbial-associated serum metabolites. The abscissa of the ROC curve is the false-positive rate; the ordinate is the true positive rate; the blue curve is the average curve after 10 folds; the AUC is the area under the curve; the shaded region is the upper and lower 1 standard deviation.

correlated with total protein (TP), platelets (PLTs), and immune cells such as LYs, indicating that HCC-related metabolites were closely related to the deterioration of liver function in HCC patients.

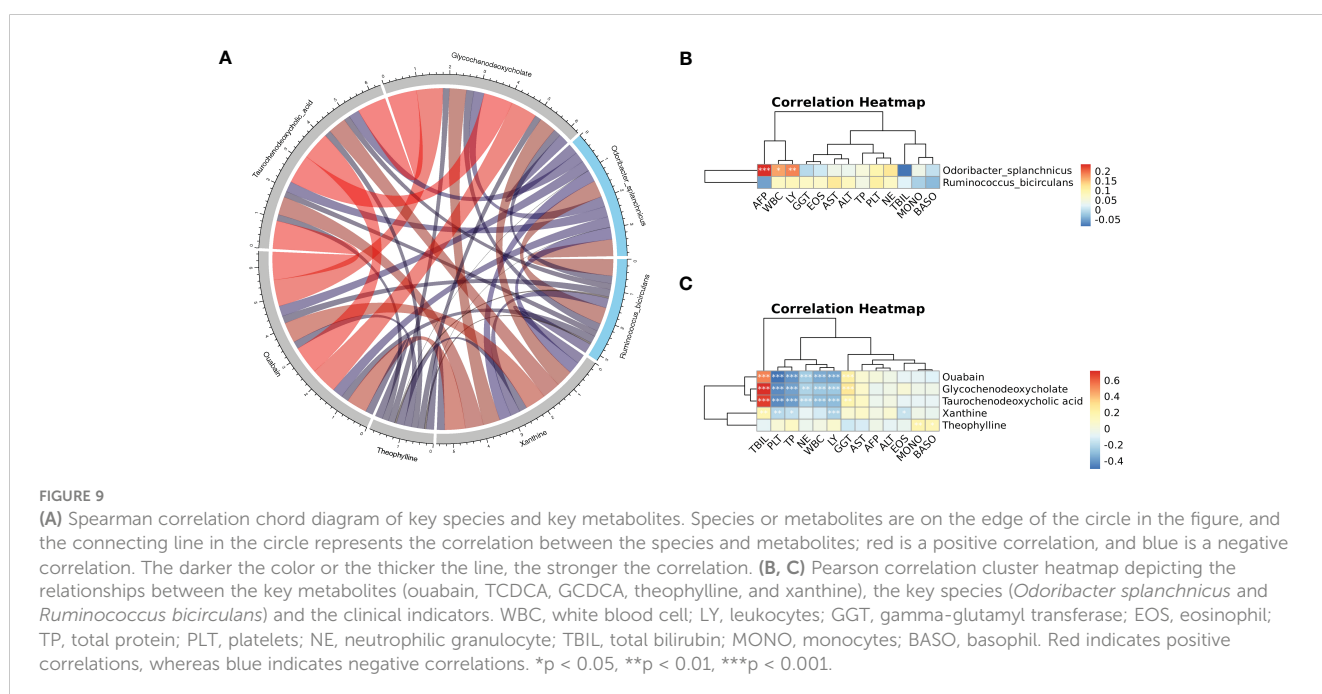
Discussion

The study's findings confirmed changes in gut microbiota and serum metabolites in HCC patients. The panels of key species and key metabolites associated with HCC as potential markers of HCC were created, both individually and in combination, and then tested the diagnostic value of each panel for HCC. By comparing the two omics to assess the diagnostic performance of different omics alone and in combination. The control group consisted of individuals who underwent a physical examination at Nanjing's Second Hospital, whereas the HCC patients were newly diagnosed patients. Study participants were screened for pharmacological factors such as anticancer drugs and antibiotics to rule out any interference with changes in the intestinal flora. It was discovered that the differences in gut microbial composition and structure among NC, HCC, and LC and the diversity of fecal microbes decreased in that order, which is consistent with previous research (Ren et al., 2019).

Fecal *Bacteroides* are a sign of a healthy gut because they break down polysaccharides and oligosaccharides and give nutrients and vitamins to the host and other intestinal microbes (Wexler, 2007). *Bacteroides acidifaciens* in the mouse intestine alleviated liver injury by reducing hepatocyte apoptosis in a cd95-dependent manner, according to one study (Wang et al., 2022a). However, it was discovered in another study on the combined gut microbial and transcriptomic analysis of HCC patients that the extent of tumor load was positively correlated with the abundance of *Bacteroides*, which caused adverse clinical outcomes via increased serum bile acids (Huang et al., 2020). Furthermore, *Bacteroides* has been

shown to be a drug target for certain herbal and anticancer drugs in the treatment of HCC, although whether by increasing or decreasing it remains debatable. The Shaoyao Ruangan Mixture, for example, may have antihepatocellular effects by increasing *Bacteroides*, whereas nimbolide has antihepatocellular effects by decreasing *Bacteroides* (Zhen et al., 2019; Ram et al., 2022). It was hypothesized that these disparities are due to differences in animal and human flora, subject selection criteria and heterogeneity, or 16S rRNA sequencing limitations. The detection of species levels is also limited by 16S rRNA sequencing, and while some microbes may maintain dynamic equilibrium at the genus level, species levels within the genus have different effects on disease susceptibility. Metagenome sequencing results revealed that differential species under the *Bacteroides* branch, such as *Bacteroides*_sp. HF-5287, *Bacteroides*_sp. A1C1, *Bacteroides*_sp. CACC_737, *Bacteroides*_sp. PHL_2737, *Bacteroides intestinalis*, *Bacteroides uniformis*, and *Bacteroides cellulolyticus* were all higher in the NC group than in the other two groups and were also important markers to distinguish the healthy group from the other two groups.

Veillonella was found to be associated with autoimmune hepatitis (AIH), primary biliary cholangitis (PBC), primary sclerosing cholangitis (PSC), HBV infection, and alcoholic hepatitis, among other liver diseases that are highly correlated with liver function indicators and liver inflammation, according to previous research (Wei et al., 2020; Kim et al., 2021). *Veillonella* was also found to be positively related to AFP, a clinical indicator of HCC (Zhang et al., 2019). This is consistent with this study that, with the exception of *Veillonella parvula*, *Veillonella* sp. T1-7, *Veillonella atypica*, *Veillonella dispar*, and most key species differing in HCC and LC had a decreasing trend compared to NC. It was also discovered that these four species were more abundant in LC than in HCC, which is consistent with the findings of a study on the gut flora of HBV-associated early HCC



and LC (Tang et al., 2021). It is worth noting that the LEfSe analysis results indicate that these four species have the potential to diagnose LC.

Furthermore, *Ruminococcus bicirculans* and *Odoribacter splanchnicus* were identified as potential species-level microbial markers for the diagnosis of HCC in the LEfSe analysis. *Ruminococcus*'s benefits and drawbacks are debatable. It has been proposed that it is a probiotic that could benefit HCC patients receiving anti-PD-1 immunotherapy as well as combat the anxiety and fear associated with cancer treatment and recurrence (Okubo et al., 2020; Mao et al., 2021). *Ruminococcus*, on the other hand, was strongly associated with some diseases and significantly enriched in patients with thyroid cancer, endometrial cancer, and clear cell renal cell carcinoma, and it may serve as a biomarker for clinical features and prognosis and provide a new therapeutic target for clinical treatment (Chen et al., 2022; Ishaq et al., 2022; Zhao et al., 2022). In this study, it was discovered that the relative abundances of *Ruminococcus* and *Ruminococcus bicirculans* in HCC were significantly lower than those in NC but significantly higher than those in LC.

In contrast, *Odoribacter splanchnicus*, another potential HCC marker, is widely regarded as a probiotic that can be used in fecal transplantation to treat disease (Lima et al., 2022). *Odoribacter splanchnicus* was found to be age-enriched in centenarians, and it may aid in health maintenance (Wang et al., 2022b). *Odoribacter splanchnicus* was shown to be useful in treating colitis and colorectal cancer by stimulating IL-6 and IL-1 production and Th17 cell expansion (Xing et al., 2021). *Odoribacter splanchnicus* was found in this study to be significantly lower in HCC and LC than in NC, and it is expected to be a new therapeutic target for HCC.

Metabolic pathway enrichment analysis was performed using differential metabolites to learn the mechanisms of the metabolic pathway changes in the different groups. Bile secretion, cholesterol metabolism, and caffeine metabolism pathways were found to be enriched in HCC versus LC, HCC versus NC, and LC versus NC, which are closely related to HCC progression. Among the various endogenous metabolites from the host intestinal flora that are synergistically metabolized, bile acids have received increased attention due to their known pro-tumorigenic properties (Quante et al., 2012; Yoshimoto et al., 2013), which involve two important receptors: the farnesoid X receptor (FXR) and the G-protein-coupled bile acid receptor (TGR5) (Jia et al., 2018). There is accumulating evidence that bile acids play an important role in HCC. TCDCA and GCDCA were discovered to be involved in the bile secretion and cholesterol metabolism pathways, and their serum concentrations were both significantly different in pairwise comparisons, suggesting that they could be used as clinical biomarkers. Previous research has discovered that TCDCA not only causes oxidative stress in gastrointestinal tumors, resulting in compensatory upregulation of TR mRNA (Lechner et al., 2002), but it also reduces expression of the tumor suppressor gene CEBP in HepG2 cell lines (Xie et al., 2016), which is correlated with the risk of colon cancer and HCC (Kühn et al., 2020; Farhat et al., 2022).

GCDCA is a significant human bile salt. GCDCA treatment of HepG2 cell lines activates ERK1 and ERK2, induces phosphorylation of Mcl-1 at the T163 site and is a potential

carcinogen in the development of HCC (Liao et al., 2011). Meanwhile, *in vitro* and *in vivo* studies revealed that GCDCA activated autophagy in HCC cells and significantly increased their invasive potential (Gao et al., 2019). These mechanisms may represent a novel treatment for HCC. TCDCA and GCDCA were significantly higher in the HCC group than in the NC group in our study.

Another important pathway involving theophylline and xanthine is caffeine metabolism. In the majority of observational studies and meta-analyses, coffee consumption has been linked to a lower risk of cancers such as colorectal (Mackintosh et al., 2020), breast (Oh et al., 2015), prostate (Wilson et al., 2011), and liver cancer (Inoue and Tsugane, 2019). Theophylline is a xanthine derivative that is primarily eliminated by liver metabolism and is used to treat respiratory diseases such as asthma. Studies have shown that increasing coffee consumption raises serum levels of the metabolite theophylline, which has been shown to have anticancer activity and a protective effect against cisplatin-induced GFR damage in patients with various malignancies, although the precise mechanism is unknown (Benoehr et al., 2005; Guertin et al., 2015). Theophylline is a natural substance that is easily accessible. It has the potential to be modified and used as a scaffold structure for the creation of effective antitumor medications. Non-small cell lung cancer (NSCLC) has been reported to be effectively treated with theophylline derivatives containing 1,2,3-triazole rings (Ye et al., 2021). According to this study, theophylline was significantly reduced in patients with HCC.

Additionally, we discovered that 9 serum metabolites, including TCDCA, GCDCA, and xanthine, were closely related to the previously screened key species *Odoribacter splanchnicus* and *Ruminococcus bicirculans* and that the KGMSM panel constructed from the 9 differential metabolites associated with the key species has some diagnostic potential. The Spearman correlation test showed that ouabain, TCDCA, GCDCA, and xanthine all had significant negative correlations with *Odoribacter splanchnicus* and *Ruminococcus bicirculans*.

Previous research has shown that both gut microbes and serum metabolites have great potential for disease diagnosis (Luo et al., 2018). However, the causal relationship between gut microbes and metabolites in HCC is unclear, and no articles have been published that report on which is best for diagnosing HCC: gut microbes or metabolites. ROC curves were used to assess each panel's potential contribution to predicting HCC, and it was found that the KSM panel was superior to the KGM panel in distinguishing HCC from non-HCC but it had an AUC value of less than 0.7 in distinguishing HCC from LC. When the KGM+KSM panel was used for the diagnosis of HCC, the AUC values for HCC versus LC (AUC > 0.7) and HCC versus NC improved, indicating that the KGM+KSM panel is superior to the KGM panel and the KSM panel as a potential marker for HCC. Using the best ROC results from separate omics modeling versus combined data modeling, the AUCs for HCC versus LC and HCC versus LC were 0.800 (merged) and 1.000 (metabolites), which are very close to the corresponding AUC values of 0.72 and 0.97 for our KGM+KSM panel. Furthermore, when the clinical indicator AFP was included in the panel, the AUC values reached 0.76 and 0.99. This study

suggest that the KGM+KSM panel could be a promising, noninvasive HCC detection method.

It is worth noting that although the changes and associations of the microbiome and metabolome in HCC were described in our study, which evaluated and compared different panels as HCC markers, these results were not validated in a separate population cohort. In the future, more and larger cohort studies will be needed.

Meanwhile, this study has some limitations. First, the prognosis is an important aspect of disease research. We were unable to study the disease's prognosis for the time being because it was not possible to follow all patients in the short term. Second, the strict enrollment criteria resulted in a small number of patients being enrolled. In the future, we hope to increase the sample size and conduct additional studies through multicenter collaboration. Finally, we focused on two HCC-related key species and five HCC-related key metabolites. We discovered their possible involvement in HCC through pathway enrichment analysis, but this needs to be validated *in vivo* and *in vitro* experiments, and we will continue our research in this direction in the future. We hope that our research will lead to new approaches to the diagnosis and treatment of HCC.

Conclusions

The intestinal flora and serum metabolism in HCC patients were studied. The results imply that HCC could be caused by a mutual regulation of key species and key metabolites. A comparison of the diagnostic performance of the KGM, KSM, and KGM + KSM panels and AFP suggested that HCC-related key species (*Odoribacter splanchnicus* and *Ruminococcus bicirculans*) and key metabolites (ouabain, TCDCA, GCDCA, theophylline, and xanthine) may be potential markers for the diagnosis of hepatocellular carcinoma.

Data availability statement

The datasets presented in this study can be found in online repositories. The names of the repository/repositories and accession number(s) can be found below: <https://ngdc.cnpc.ac.cn/gsa-human/s/b1n2unmw>, metagenome sequencing; <https://ngdc.cnpc.ac.cn/omix/preview/46n71k8z>, metabolomics.

References

- Al-Zoughbi, W., Al-Zoughbi, W., Huang, J., Paramasivan, G. S., Till, H., Pichler, M., et al. (2014). Tumor macroenvironment and metabolism. *Semin. Oncol.* 41 (2), 281–295. doi: 10.1053/j.seminoncol.2014.02.005
- Anand, S., Kaur, H., and Mande, S. S. (2016). Comparative in silico analysis of butyrate production pathways in gut commensals and pathogens. *Front. Microbiol.* 7. doi: 10.3389/fmicb.2016.01945
- European Association for the Study of the Liver. (2022). EASL clinical practice guidelines on haemochromatosis. *J. Hepatol.* 77 (2), 479–502. doi: 10.1016/j.jhep.2022.03.033

Ethics statement

The studies involving human participants were reviewed and approved by The Medical ethics committee of The Second Hospital of Nanjing. The patients/participants provided their written informed consent to participate in this study.

Author contributions

XL conducted all experiments and wrote the manuscript. XL and XG collected samples. YY and HJ revised the manuscript. All authors contributed to the article and approved the submitted version.

Funding

This study was supported by funding for the Infectious Disease Clinical Center of Nanjing, the Infectious Disease Innovation Center of Jiangsu, and Jiangsu Province Postgraduate Research and Practice Innovation Program of Nanjing University of Chinese Medicine (Grant No. KYCX22_2069).

Conflict of interest

The authors declare that the research was conducted in the absence of any commercial or financial relationships that could be construed as a potential conflict of interest.

Publisher's note

All claims expressed in this article are solely those of the authors and do not necessarily represent those of their affiliated organizations, or those of the publisher, the editors and the reviewers. Any product that may be evaluated in this article, or claim that may be made by its manufacturer, is not guaranteed or endorsed by the publisher.

Supplementary material

The Supplementary Material for this article can be found online at: <https://www.frontiersin.org/articles/10.3389/fcimb.2023.1170748/full#supplementary-material>

- Bajaj, J. S., Heuman, D. M., Hylemon, P. B., Sanyal, A. J., White, M. B., Monteith, P., et al. (2014). Altered profile of human gut microbiome is associated with cirrhosis and its complications. *J. Hepatol.* 60 (5), 940–947. doi: 10.1016/j.jhep.2013.12.019
- Benoehr, P., Krueth, P., Bokemeyer, C., Grenz, A., Osswald, H., and Hartmann, J. T. (2005). Nephroprotection by theophylline in patients with cisplatin chemotherapy: a randomized, single-blinded, placebo-controlled trial. *J. Am. Soc. Nephrol.* 16 (2), 452–458. doi: 10.1681/asn.2004030225
- Beyoğlu, D., and Idle, J. R. (2013). The metabolomic window into hepatobiliary disease. *J. Hepatol.* 59 (4), 842–858. doi: 10.1016/j.jhep.2013.05.030

- Bray, F., Ferlay, J., Soerjomataram, I., Siegel, R. L., Torre, L. A., and Jemal, A. (2018). Global cancer statistics 2018: GLOBOCAN estimates of incidence and mortality worldwide for 36 cancers in 185 countries. *CA Cancer J. Clin.* 68 (6), 394–424. doi: 10.3322/caac.21492
- Buchfink, B., Xie, C., and Huson, D. H. (2015). Fast and sensitive protein alignment using DIAMOND. *Nat. Methods* 12 (1), 59–60. doi: 10.1038/nmeth.3176
- Chen, Y., Ma, J., Dong, Y., Yang, Z., Zhao, N., Liu, Q., et al. (2022). Characteristics of gut microbiota in patients with clear cell renal cell carcinoma. *Front. Microbiol.* 13. doi: 10.3389/fmicb.2022.913718
- Dodd, D., Spitzer, M. H., Van Treuren, W., Merrill, B. D., Hryckowian, A. J., Higginbottom, S. K., et al. (2017). A gut bacterial pathway metabolizes aromatic amino acids into nine circulating metabolites. *Nature* 551 (7682), 648–652. doi: 10.1038/nature24661
- Dunn, W. B., Broadhurst, D., Begley, P., Zelena, E., Francis-McIntyre, S., Anderson, N., et al. (2011). Procedures for large-scale metabolic profiling of serum and plasma using gas chromatography and liquid chromatography coupled to mass spectrometry. *Nat. Protoc.* 6 (7), 1060–1083. doi: 10.1038/nprot.2011.335
- Farhat, Z., Freedman, N. D., Sampson, J. N., Falk, R. T., Koshiol, J., Weinstein, S. J., et al. (2022). A prospective investigation of serum bile acids with risk of liver cancer, fatal liver disease, and biliary tract cancer. *Hepatol. Commun.* 6 (9), 2391–2399. doi: 10.1002/hep4.2003
- Fausto, N., Campbell, J. S., and Riehle, K. J. (2006). Liver regeneration. *Hepatology* 43 (2 Suppl 1), S45–S53. doi: 10.1002/hep.20969
- Fu, L., Niu, B., Zhu, Z., Wu, S., and Li, W. (2012). CD-HIT: accelerated for clustering the next-generation sequencing data. *Bioinformatics* 28 (23), 3150–3152. doi: 10.1093/bioinformatics/bts565
- Gao, L., Lv, G., Li, R., Liu, W. T., Zong, C., Ye, F., et al. (2019). Glycochenodeoxycholate promotes hepatocellular carcinoma invasion and migration by AMPK/mTOR dependent autophagy activation. *Cancer Lett.* 454, 215–223. doi: 10.1016/j.canlet.2019.04.009
- Guertin, K. A., Lofffield, E., Boca, S. M., Sampson, J. N., Moore, S. C., Xiao, Q., et al. (2015). Serum biomarkers of habitual coffee consumption may provide insight into the mechanism underlying the association between coffee consumption and colorectal cancer. *Am. J. Clin. Nutr.* 101 (5), 1000–1011. doi: 10.3945/ajcn.114.096099
- Huang, H., Ren, Z., Gao, X., Hu, X., Zhou, Y., Jiang, J., et al. (2020). Integrated analysis of microbiome and host transcriptome reveals correlations between gut microbiota and clinical outcomes in HBV-related hepatocellular carcinoma. *Genome Med.* 12 (1), 102. doi: 10.1186/s13073-020-00796-5
- Inoue, M., and Tsugane, S. (2019). Coffee drinking and reduced risk of liver cancer: update on epidemiological findings and potential mechanisms. *Curr. Nutr. Rep.* 8 (3), 182–186. doi: 10.1007/s13668-019-0274-1
- Ishaq, H. M., Mohammad, I. S., Hussain, R., Parveen, R., Shirazi, J. H., Fan, Y., et al. (2022). Gut-thyroid axis: how gut microbial dysbiosis associated with euthyroid thyroid cancer. *J. Cancer* 13 (6), 2014–2028. doi: 10.7150/jca.66816
- Jia, W., Xie, G., and Jia, W. (2018). Bile acid-microbiota crosstalk in gastrointestinal inflammation and carcinogenesis. *Nat. Rev. Gastroenterol. Hepatol.* 15 (2), 111–128. doi: 10.1038/nrgastro.2017.119
- Kim, S. S., Eun, J. W., Cho, H. J., Song, D. S., Kim, C. W., Kim, Y. S., et al. (2021). Microbiome as a potential diagnostic and predictive biomarker in severe alcoholic hepatitis. *Aliment. Pharmacol. Ther.* 53 (4), 540–551. doi: 10.1111/apt.16200
- Kobayashi, T., Aikata, H., Kobayashi, T., Ohdan, H., Arihiro, K., and Chayama, K. (2017). Patients with early recurrence of hepatocellular carcinoma have poor prognosis. *Hepatobiliary Pancreat. Dis. Int.* 16 (3), 279–288. doi: 10.1016/j.hpb.2016.01.018-9
- Kühn, T., Stepien, M., López-Nogueroles, M., Damms-Machado, A., Sookthai, D., Johnson, T., et al. (2020). Prediagnostic plasma bile acid levels and colon cancer risk: a prospective study. *J. Natl. Cancer Inst.* 112 (5), 516–524. doi: 10.1093/jnci/djz166
- Langmead, B., and Salzberg, S. L. (2012). Fast gapped-read alignment with bowtie 2. *Nat. Methods* 9 (4), 357–359. doi: 10.1038/nmeth.1923
- Lechner, S., Müller-Ladner, U., Schlottmann, K., Jung, B., McClelland, M., Rüschoff, J., et al. (2002). Bile acids mimic oxidative stress induced upregulation of thioredoxin reductase in colon cancer cell lines. *Carcinogenesis* 23 (8), 1281–1288. doi: 10.1093/carcin/23.8.1281
- Li, R., Li, Y., Kristiansen, K., and Wang, J. (2008). SOAP: short oligonucleotide alignment program. *Bioinformatics* 24 (5), 713–714. doi: 10.1093/bioinformatics/btn025
- Li, D., Liu, C. M., Luo, R., Sadakane, K., and Lam, T. W. (2015). MEGAHIT: an ultra-fast single-node solution for large and complex metagenomics assembly via succinct de bruijn graph. *Bioinformatics* 31 (10), 1674–1676. doi: 10.1093/bioinformatics/btv033
- Liao, M., Zhao, J., Wang, T., Duan, J., Zhang, Y., and Deng, X. (2011). Role of bile salt in regulating mcl-1 phosphorylation and chemoresistance in hepatocellular carcinoma cells. *Mol. Cancer* 10, 44. doi: 10.1186/1476-4598-10-44
- Lima, S. F., Gogokhia, L., Viladomiu, M., Chou, L., Putzel, G., Jin, W. B., et al. (2022). Transferable immunoglobulin a-coated oridobacter splanchnicus in responders to fecal microbiota transplantation for ulcerative colitis limits colonic inflammation. *Gastroenterology* 162 (1), 166–178. doi: 10.1053/j.gastro.2021.09.061
- Liu, J., Geng, W., Sun, H., Liu, C., Huang, F., Cao, J., et al. (2022). Integrative metabolomic characterisation identifies altered portal vein serum metabolome contributing to human hepatocellular carcinoma. *Gut* 71 (6), 1203–1213. doi: 10.1136/gutjnl-2021-325189
- Louis, P., Hold, G. L., and Flint, H. J. (2014). The gut microbiota, bacterial metabolites and colorectal cancer. *Nat. Rev. Microbiol.* 12 (10), 661–672. doi: 10.1038/nrmicro3344
- Lucas, C., Barnich, N., and Nguyen, H. T. T. (2017). Microbiota, inflammation and colorectal cancer. *Int. J. Mol. Sci.* 18 (6). doi: 10.3390/ijms18061310
- Luo, P., Yin, P., Hua, R., Tan, Y., Li, Z., Qiu, G., et al. (2018). A Large-scale, multicenter serum metabolite biomarker identification study for the early detection of hepatocellular carcinoma. *Hepatology* 67 (2), 662–675. doi: 10.1002/hep.29561
- Mackintosh, C., Yuan, C., Ou, F. S., Zhang, S., Niedzwiecki, D., Chang, I. W., et al. (2020). Association of coffee intake with survival in patients with advanced or metastatic colorectal cancer. *JAMA Oncol.* 6 (11), 1713–1721. doi: 10.1001/jamaoncol.2020.3938
- Mao, J., Wang, D., Long, J., Yang, X., Lin, J., Song, Y., et al. (2021). Gut microbiome is associated with the clinical response to anti-PD-1 based immunotherapy in hepatobiliary cancers. *J. Immunother. Cancer* 9 (12). doi: 10.1136/jitc-2021-003334
- Marrero, J. A., and Lok, A. S. (2004). Newer markers for hepatocellular carcinoma. *Gastroenterology* 127 (5 Suppl 1), S113–S119. doi: 10.1053/j.gastro.2004.09.024
- O'Keefe, S. J. (2016). Diet, microorganisms and their metabolites, and colon cancer. *Nat. Rev. Gastroenterol. Hepatol.* 13 (12), 691–706. doi: 10.1038/nrgastro.2016.165
- Oh, J. K., Sandin, S., Ström, P., Löf, M., Adami, H. O., and Weiderpass, E. (2015). Prospective study of breast cancer in relation to coffee, tea and caffeine in Sweden. *Int. J. Cancer* 137 (8), 1979–1989. doi: 10.1002/ijc.29569
- Okubo, R., Kinoshita, T., Katsumata, N., Uezono, Y., Xiao, J., and Matsuoka, Y. J. (2020). Impact of chemotherapy on the association between fear of cancer recurrence and the gut microbiota in breast cancer survivors. *Brain Behav. Immun.* 85, 186–191. doi: 10.1016/j.bbi.2019.02.025
- Patel, S., and Ahmed, S. (2015). Emerging field of metabolomics: big promise for cancer biomarker identification and drug discovery. *J. Pharm. BioMed. Anal.* 107, 63–74. doi: 10.1016/j.jpba.2014.12.020
- Patro, R., Duggal, G., Love, M. I., Irizarry, R. A., and Kingsford, C. (2017). Salmon provides fast and bias-aware quantification of transcript expression. *Nat. Methods* 14 (4), 417–419. doi: 10.1038/nmeth.4197
- Ponziani, F. R., Bhoori, S., Castelli, C., Putignani, L., Rivoltini, L., Del Chierico, F., et al. (2019). Hepatocellular carcinoma is associated with gut microbiota profile and inflammation in nonalcoholic fatty liver disease. *Hepatology* 69 (1), 107–120. doi: 10.1002/hep.30036
- Qin, J., Li, Y., Cai, Z., Li, S., Zhu, J., Zhang, F., et al. (2012). A metagenome-wide association study of gut microbiota in type 2 diabetes. *Nature* 490 (7418), 55–60. doi: 10.1038/nature11450
- Quante, M., Bhagat, G., Abrams, J. A., Marache, F., Good, P., Lee, M. D., et al. (2012). Bile acid and inflammation activate gastric cardia stem cells in a mouse model of Barrett-like metaplasia. *Cancer Cell* 21 (1), 36–51. doi: 10.1016/j.ccr.2011.12.004
- Ram, A. K., Vairappan, B., and Srinivas, B. H. (2022). Nimbolide attenuates gut dysbiosis and prevents bacterial translocation by improving intestinal barrier integrity and ameliorating inflammation in hepatocellular carcinoma. *Phytother. Res.* 36 (5), 2143–2160. doi: 10.1002/ptr.7434
- Ren, Z., Jiang, J., Xie, H., Li, A., Lu, H., Xu, S., et al. (2017). Gut microbial profile analysis by MiSeq sequencing of pancreatic carcinoma patients in China. *Oncotarget* 8 (56), 95176–95191. doi: 10.18632/oncotarget.18820
- Ren, Z., Li, A., Jiang, J., Zhou, L., Yu, Z., Lu, H., et al. (2019). Gut microbiome analysis as a tool towards targeted non-invasive biomarkers for early hepatocellular carcinoma. *Gut* 68 (6), 1014–1023. doi: 10.1136/gutjnl-2017-315084
- Sarafian, M. H., Gaudin, M., Lewis, M. R., Martin, F. P., Holmes, E., Nicholson, J. K., et al. (2014). Objective set of criteria for optimization of sample preparation procedures for ultra-high throughput untargeted blood plasma lipid profiling by ultra performance liquid chromatography-mass spectrometry. *Anal. Chem.* 86 (12), 5766–5774. doi: 10.1021/ac500317c
- Shen, F., Zheng, R. D., Sun, X. Q., Ding, W. J., Wang, X. Y., and Fan, J. G. (2017). Gut microbiota dysbiosis in patients with non-alcoholic fatty liver disease. *Hepatobiliary Pancreat. Dis. Int.* 16 (4), 375–381. doi: 10.1016/s1499-3872(17)60019-5
- Stat, M., Pochon, X., Franklin, E. C., Bruno, J. F., Casey, K. S., Selig, E. R., et al. (2013). The distribution of the thermally tolerant symbiont lineage (Symbiodinium clade D) in corals from Hawaii: correlations with host and the history of ocean thermal stress. *Ecol. Evol.* 3 (5), 1317–1329. doi: 10.1002/ece3.556
- Tang, Y., Zhou, H., Xiang, Y., and Cui, F. (2021). The diagnostic potential of gut microbiome for early hepatitis b virus-related hepatocellular carcinoma. *Eur. J. Gastroenterol. Hepatol.* 33 (1S Suppl 1), e167–e175. doi: 10.1097/meg.0000000000001978
- Tong, M., Wong, T. L., Zhao, H., Zheng, Y., Xie, Y. N., Li, C. H., et al. (2021). Loss of tyrosine catabolic enzyme HPD promotes glutamine anaplerosis through mTOR signaling in liver cancer. *Cell Rep.* 37 (5), 109976. doi: 10.1016/j.celrep.2021.109976
- Torre, L. A., Bray, F., Siegel, R. L., Ferlay, J., Lortet-Tieulent, J., and Jemal, A. (2015). Global cancer statistic. *CA Cancer J. Clin.* 65 (2), 87–108. doi: 10.3322/caac.21262
- Tripathi, A., Debelius, J., Brenner, D. A., Karin, M., Loomba, R., Schnabl, B., et al. (2018). The gut-liver axis and the intersection with the microbiome. *Nat. Rev. Gastroenterol. Hepatol.* 15 (7), 397–411. doi: 10.1038/s41575-018-0011-z

- Vander Heiden, M. G., and DeBerardinis, R. J. (2017). Understanding the intersections between metabolism and cancer biology. *Cell* 168 (4), 657–669. doi: 10.1016/j.cell.2016.12.039
- Wang, J., Qie, J., Zhu, D., Zhang, X., Zhang, Q., Xu, Y., et al. (2022b). The landscape in the gut microbiome of long-lived families reveals new insights on longevity and aging - relevant neural and immune function. *Gut Microbes* 14 (1), 2107288. doi: 10.1080/19490976.2022.2107288
- Wang, H., Wang, Q., Yang, C., Guo, M., Cui, X., Jing, Z., et al. (2022a). Bacteroides acidifaciens in the gut plays a protective role against CD95-mediated liver injury. *Gut Microbes* 14 (1), 2027853. doi: 10.1080/19490976.2022.2027853
- Wei, Y., Li, Y., Yan, L., Sun, C., Miao, Q., Wang, Q., et al. (2020). Alterations of gut microbiome in autoimmune hepatitis. *Gut* 69 (3), 569–577. doi: 10.1136/gutjnl-2018-317836
- Wen, B., Mei, Z., Zeng, C., and Liu, S. (2017). metaX: a flexible and comprehensive software for processing metabolomics data. *BMC Bioinf.* 18 (1), 183. doi: 10.1186/s12859-017-1579-y
- Wexler, H. M. (2007). Bacteroides: the good, the bad, and the nitty-gritty. *Clin. Microbiol. Rev.* 20 (4), 593–621. doi: 10.1128/cmr.00008-07
- Wilson, K. M., Kasperzyk, J. L., Rider, J. R., Kenfield, S., van Dam, R. M., Stampfer, M. J., et al. (2011). Coffee consumption and prostate cancer risk and progression in the health professionals follow-up study. *J. Natl. Cancer Inst.* 103 (11), 876–884. doi: 10.1093/jnci/djr151
- Xie, G., Wang, X., Huang, F., Zhao, A., Chen, W., Yan, J., et al. (2016). Dysregulated hepatic bile acids collaboratively promote liver carcinogenesis. *Int. J. Cancer* 139 (8), 1764–1775. doi: 10.1002/ijc.30219
- Xing, C., Wang, M., Ajibade, A. A., Tan, P., Fu, C., Chen, L., et al. (2021). Microbiota regulate innate immune signaling and protective immunity against cancer. *Cell Host Microbe* 29 (6), 959–974.e957. doi: 10.1016/j.chom.2021.03.016
- Ye, J., Mao, L., Xie, L., Zhang, R., Liu, Y., Peng, L., et al. (2021). Discovery of a series of theophylline derivatives containing 1,2,3-triazole for treatment of non-small cell lung cancer. *Front. Pharmacol.* 12. doi: 10.3389/fphar.2021.753676
- Yoshimoto, S., Loo, T. M., Atarashi, K., Kanda, H., Sato, S., Oyadomari, S., et al. (2013). Obesity-induced gut microbial metabolite promotes liver cancer through senescence secretome. *Nature* 499 (7456), 97–101. doi: 10.1038/nature12347
- Yu, J., Feng, Q., Wong, S. H., Zhang, D., Liang, Q. Y., Qin, Y., et al. (2017). Metagenomic analysis of faecal microbiome as a tool towards targeted non-invasive biomarkers for colorectal cancer. *Gut* 66 (1), 70–78. doi: 10.1136/gutjnl-2015-309800
- Zhang, L., Wu, Y. N., Chen, T., Ren, C. H., Li, X., and Liu, G. X. (2019). Relationship between intestinal microbial dysbiosis and primary liver cancer. *Hepatobiliary Pancreat. Dis. Int.* 18 (2), 149–157. doi: 10.1016/j.hbpd.2019.01.002
- Zhao, S. S., Chen, L., Yang, J., Wu, Z. H., Wang, X. Y., Zhang, Q., et al. (2022). Altered gut microbial profile accompanied by abnormal fatty acid metabolism activity exacerbates endometrial cancer progression. *Microbiol. Spectr.* 10 (6), e0261222. doi: 10.1128/spectrum.02612-22
- Zhen, H., Qian, X., Fu, X., Chen, Z., Zhang, A., and Shi, L. (2019). Regulation of shaoyao ruangan mixture on intestinal flora in mice with primary liver cancer. *Integr. Cancer Ther.* 18, 1534735419843178. doi: 10.1177/1534735419843178
- Zhu, W., Lomsadze, A., and Borodovsky, M. (2010). Ab initio gene identification in metagenomic sequences. *Nucleic Acids Res.* 38 (12), e132. doi: 10.1093/nar/gkq275